Supplementary information

Oriented Bacteriorhodopsin/Polyaniline Hybrid Bio-Nanofilms as Photo-Assisted Electrodes for High Performance Supercapacitor

Haijuan Li[a], Minmin Wang[a,b], Guohua Qi[a,b], Yong Xia[a], Chuanping Li[a,b], Ping Wang[a], Mordechai Sheves[c], Yongdong Jin*[a]

Experimental section:

Materials.

Aniline monomer, H_2SO_4, KCl and $HClO_4$ were purchased from Beijing Chemical Corp. 4-aminothiophenol was purchased from J&K Chemical. Tris(hydroxymethyl)-aminomethane (Tri-HCl) was purchased from DingGuo Biotech. Ltd. (Beijing, China). Purple membrane (PM) consists of 75% bacteriorhodopsin (bR) and 25% lipid bilayer was donated by Weizmann Institute of Science. Egg phosphatidylcholine (PC) was purchased from Shanghai Advanced Vehicle Technology Pharmaceutical Ltd. Aniline was distilled before use, all other chemicals used in this work were of analytical grade and used without further purification. All aqueous solutions were prepared with ultra-pure water obtained from a Millipore System (>18 MΩ cm).

Preparation of bR-containing vesicles. Preparation of bR-Containing Vesicles was conducted according to previously reported method.[1] Typically, 20 mg egg PC was dissolved in 4 ml of 150 mM KCl and 20 mM Tris-HCl solution (pH 9.2) with three different bR content by vortex shaking. The final bR concentrations were 0.12 mg/mL for bR_{o1}, 0.25 mg/mL for bR_{o2} and 0.32 mg/mL for bR_{o3} respectively. Then the multilayered liposomes were transferred to a sonication vessel and sonicated using a tip 600 times for 3 s with 3 s intervals under 200 W in an ice bath to get unilamellar vesicles.

Modification of the gold electrode. Gold electrode with 2 mm diameter was used as the working electrode. Before modification, the electrode was polished with 1, 0.3, and 0.05 μm Al_2O_3 paste to ensure a mirror like surface. It was then ultrasonic processed in

water and ethanol for 10 min respectively. After that, the electrode was scanned in 1 M H_2SO_4 in the range from -0.2 to 1.4 V until a stable and standard cyclic voltammetry was obtained. Then, the electrode was treated with UV ozone cleaners for 30 min. The electrode was then ultrasonic processed in ethanol for 5 min and rinsed with ethanol thoroughly and immersed in 10 mM 4-ATP solution for about 4 h. After that, the electrode was rinsed with ethanol and dried with N_2.

Deposition of the PANI film. The deposition of PANI was conducted in 0.1 M aniline in 1 M H_2SO_4 aqueous solution (purged with nitrogen flow before use). The potential was scanning between - 0.2 and 0.9 V at a scan rate of 1 mV/s for one cycle.

Preparation of bR monolayer-containing lipid bilayers via vesicle fusion. The PANI electrode was immersed in bR-containing vesicles for 20 min and transferred into pH 9.2 Tris buffer solution and incubated for 4 h to ensure vesicle fusion. After slight sonicating (10 s with 20 s intervals, 100 W) in a bath for about 2 min, the sample was dried by N_2 and was then ready for characterizations.

Estimation of actual occupied area of bR in the as-prepared bR monolayers. For typical bR_{o3} film, the ratio of bR to egg PC was calculated to measure the area (surface coverage) that bR molecular occupied. Native purple membrane (PM) consists of 75% bR and 25% lipid bilayer, the molecule ratio of bR to PC is about 1 to 11.6. The dimension of a unit PM (with one bR trimer) is about 6.2 nm with the area about 30.18 nm^2, while one PC lipid possess about 0.75 nm^2 footprint, so bR occupied 21.48 nm^2 in one PM unit. For 0.32 mg/mL bR_{o3} (MW=26000) and 5 mg/mL egg PC (MW=750), the molar concentrations are 1.23×10^{-5} M and 6.67×10^{-3} M, respectively. The area ratio of bR to PC is about $1.23\times10^{-5}\times21.48$ nm^2 to $6.67\times10^{-3}\times0.75$ nm^2, equals 0.053. So for a bR-modified 1 cm$\times$1 cm electrode, prepared by vesicle fusion technique, the actual occupied area by bR is about 0.05 cm^2.

Quartz crystal microbalance (QCM) measurements. The frequency responses of QCM devices in aqueous solutions is correlated to interfacial reactions involving changes in mass. Measurements were performed by using 5 MHz, AT-cut quartz crystals. The resonance frequency of the crystal was determined by using the crystal as

the frequency determining element of an electronic oscillator, the measurements being taken using a GW frequency counter, Model GFC-8055G. Details of the apparatus design and the procedures were described in earlier studies.[2] The mass per unit area of PANI film, Δm/A (g/cm^2), grown onto the gold electrode on the crystal surface was determined from the change in its resonance frequency. The following equation (Sauerbrey's equation) had been established for an AT-cut shear mode QCM to show the relation between the Δf and Δm/A. Gold resonators (0.14 cm^2) were used in these experiments.

$$\Delta f = -\left(\frac{2f_{\circ}^2}{\sqrt{\rho_Q \mu_Q}}\right)\frac{\Delta m}{A}$$

Where Δf is the measured frequency shift due to the added mass in hertz, f_o is the fundamental oscillation frequency of the dry crystal, Δm/A (g/cm^2) the mass per unit area, ρ_Q the quartz density with the value (2.649 g/cm^3) and μ_Q the shear modulus with the value (2.947×10^{11} dyne/cm^2).

Capacitance calculations. The specific capacitance (Cs) was calculated from the discharge curve according to the equation Cs = I/(m(ΔV/Δt)), where m in gram, I in ampere, ΔV in volt and Δt in second represent the mass of the electrode material, the applied current, voltage range, and discharge time, respectively.

Light-induced pH change measured by immersing bR/PANI electrode in Na_2SO_4/H_2SO_4 solution. To confirm that the proton pumping ability of bR are reserved after adsorbed on PANI film, the as-prepared oriented-bR/PANI film on ITO electrode was immersed into 4 mL Na_2SO_4/H_2SO_4 solution, then a portable pH meter was used to monitor the pH change of the solution upon light irradiation**.**

The photon flux calculation.

The photon flux was calculated by measuring the laser power (which was adjusted to a desired value and measured using a Thorlabs Digital Optical Meter – PM206) assuming that all photons had the same wavelength of 550 nm (3.57×10^{-19} Joule/photon). In this adjustment of the power we accounted for the irradiated area over the sample, as well as for the absorption of the reaction cell window and other minor losses in the setup.

The laser wavelength (λ) we used was 550 [nm]; therefore the energy each photon carries can be calculated to be:

$$(photon) = h \times c/\lambda = \frac{6.626 \times 10^{-34}[j \cdot sec] \times 3 \times 10^{8}[^{m}/_{sec}]}{550 \times 10^{-9}} = 3.57 \times 10^{-19} [^{j}/_{photon}]$$

Where h is Planck's constant and c is the speed of light.

The laser power detected by Thorlabs Digital Optical Meter was about 41 mW/cm^2, thus the photon flux (amount of photons per second) is given by:

$$Power = 41\ mW/cm^2 \rightarrow \frac{41 \times 10^{-3}[^{j}/_{cm^2 sec}]}{3.57 \times 10^{-19}[^{j}/_{photon}]} = 1.15 \times 10^{17}[^{photon}/_{cm^2 sec}]$$

Calculation of quantum efficiency of bR for the light-associated process.

The concentration of proton that bR transferred under light irradiation was calculated according to the pH change of the bR/PANI-ITO electrode (active area: about 1 cm×1 cm) in the Na_2SO_4/H_2SO_4 solution. As shown in Video S1, under 550 nm light irradiation, for the oriented-bR/PANI film electrode, the pH of 4 mL Na_2SO_4/H_2SO_4 solution decreased from 4.23 to 4.15 in about 170 s. So the light-induced H^+ content change in solution was calculated to be about ($10^{-4.15}$ - $10^{-4.23}$)mol/L ×4×10^{-3}L×6.022 ×10^{23} = 2.87 ×10^{16}[proton]. Since bR took only 0.05 cm^2 area on the 1 cm×1 cm electrode, so the QE was calculated as follows:

$$QE = \frac{2.87 \times 10^{16} proton/170 sec}{1.15 \times 10^{17}[^{photon}/_{cm^2 sec}] \times 0.05 cm^2} \sim 3.0\%$$

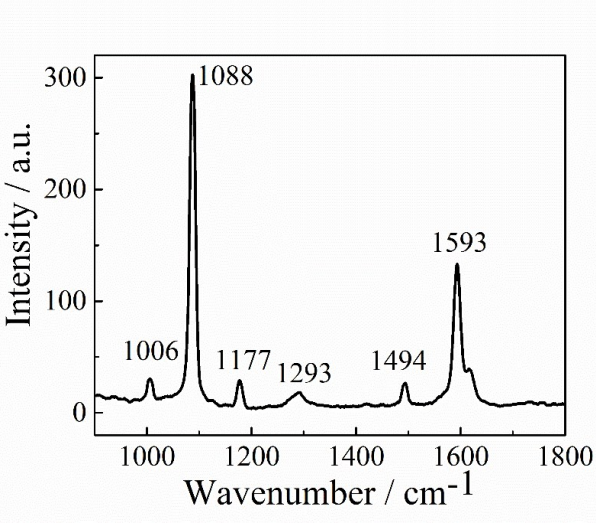

Figure S1. Raman spectrum of 4-ATP monolayer on the surface of a gold electrode.

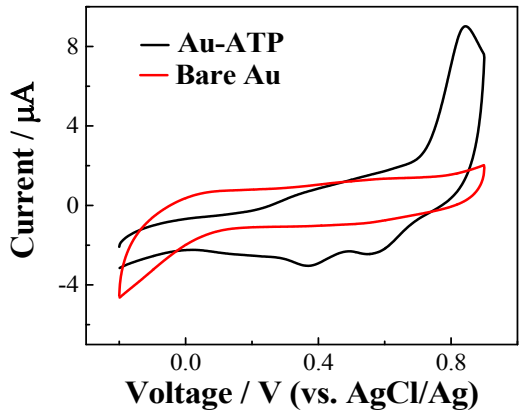

Figure S2. CV curves of 4-ATP/Au substrate (black line) and bare Au electrode (red line) in 1 M H_2SO_4 solution at a scan rate of 50 mV/s.

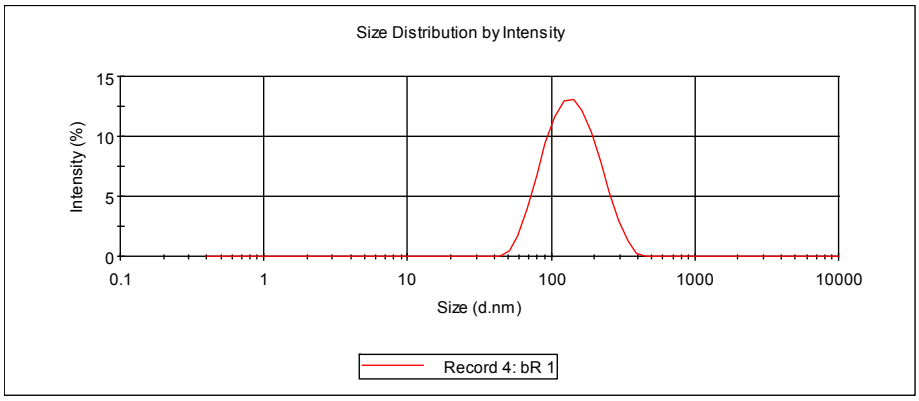

Figure S3. Hydrodynamic size of bR vesicles determined by dynamic light scattering.

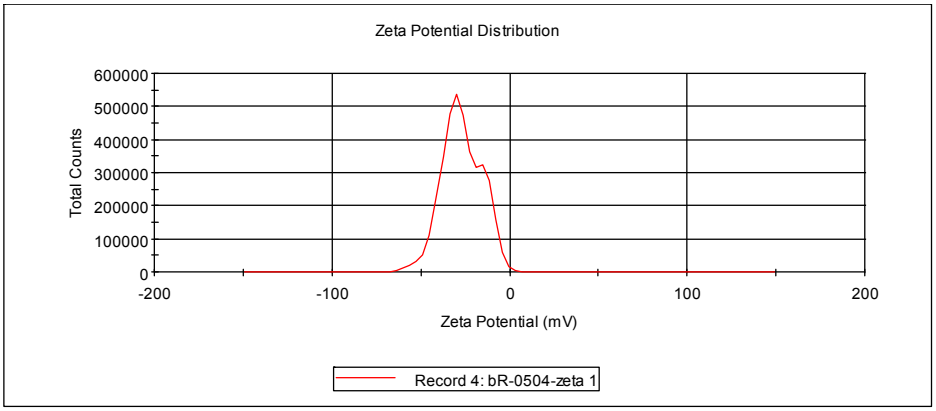

Figure S4. Zeta potential of bR vesicles determined by dynamic light scattering.

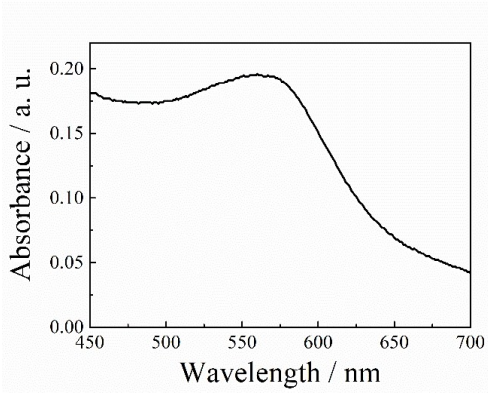

Figure S5. Absorption spectrum of the bR-incorporated vesicle suspension.

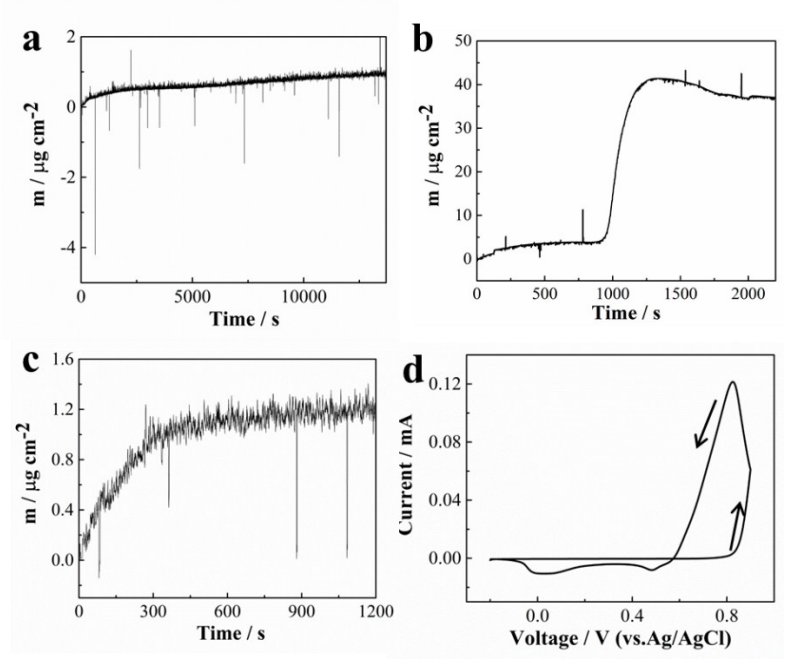

Figure S6. Mass change (calculated by QCM measurements) during the assembly of ATP on the gold electrode (a), the electrodeposition of PANI (b) and the adsorption of bR (c), CV curve for electrodeposition of PANI on gold electrode in 1 M H_2SO_4 and 0.1 M aniline (d), the scan rate is 1 mV/s.

In this work, 2 mm diameter gold electrodes were used as the working electrode throughout the experiment. The area of the working electrode is about 3.14×10^{-2} cm^2. Mass of the ATP absorbed on the surface of the gold electrode is about 8.9×10^{-2} μg. Mass of PANI deposited on the electrode is about 1.16 μg. The electropolymerization of PANI includes nucleation growth and deposition process, when the potential increased from -0.2 V to about 0.8 V, the current and the mass of the PANI increased slowly, this stage is the nucleation growth and oligomer formation stage, when the potential increased from 0.8 V to 0.9 V, both the current and the mass of PANI increased dramatically, this stage is the deposition stage, the PANI film rapidly grow, accompanied H^+ ions and SO_4^{2-} ions doping into the PANI film. When the potential backward scanned from 0.8 V to -0.2 V, the mass of the PANI decreased, indicating the dedoping of H^+ ions and SO_4^{2-} ions from the PANI film. The mass of bR vesicles adsorbed by PANI film increased rapidly in the first five minutes then gradually increase to a platform. The mass of bR vesicles adsorbed by PANI for about 20 min is

about 0.11 μg, and the pure bR is about 5.46×10^{-3} μg.

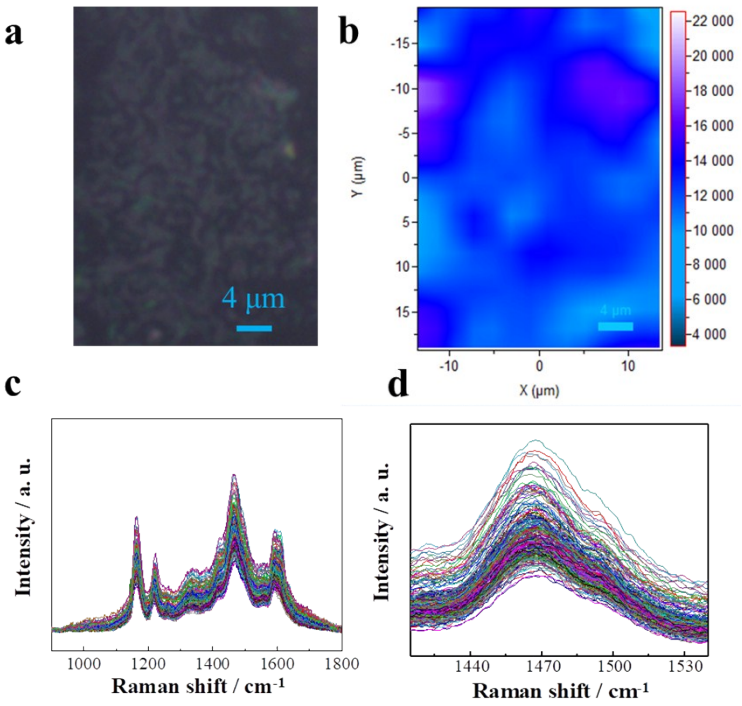

Figure S7. (a) Bright field image of bR/PANI film; (b) The Raman mapping image of bR vesicles in the bR/PANI film; (c) The Raman spectra of bR/PANI in the selected area for mapping; (d) Raman mapping is painted based on the integral area of the peak at 1470 cm^{-1} (from 1425 to 1530 cm^{-1}). This peak is corresponding to C-C-H in-plane deformation mode of the bR molecular. As shown in the Raman mapping image, the bR vesicle is mostly uniformly dispersed on the PANI film.

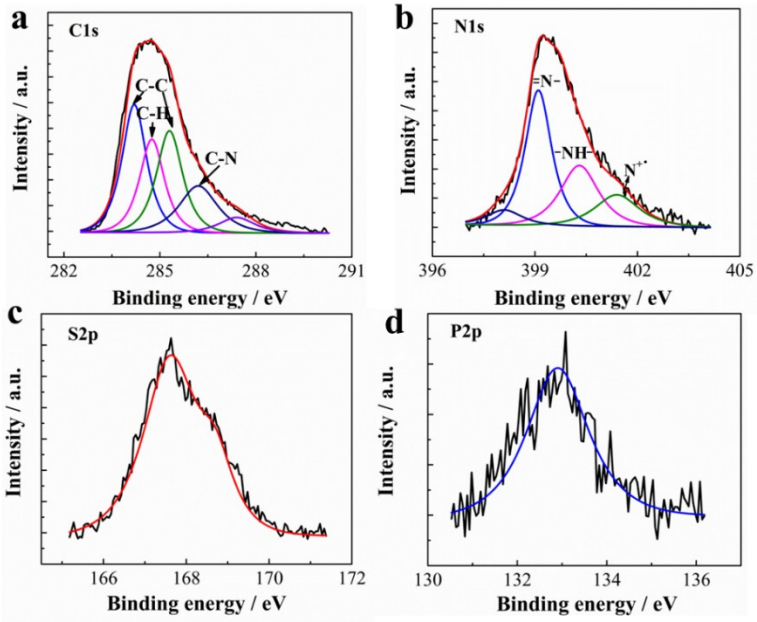

Figure S8. C1s (a), N1s (b), S 2p (c), and P 2p (d) XPS spectra of the bR/PANI.

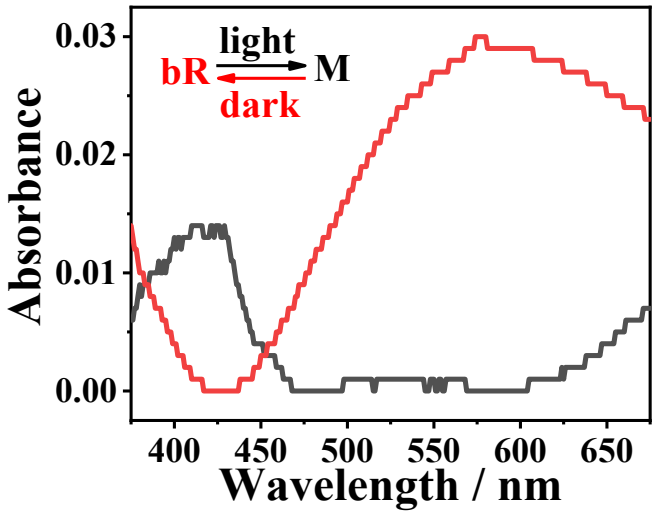

Figure S9. Difference-adsorption spectra of bR/PANI films deposited on ITO electrode, as a result of green-light irradiation. The black curve was obtained immediately after green light irradiation, and the red curve was obtained after kept in dark.

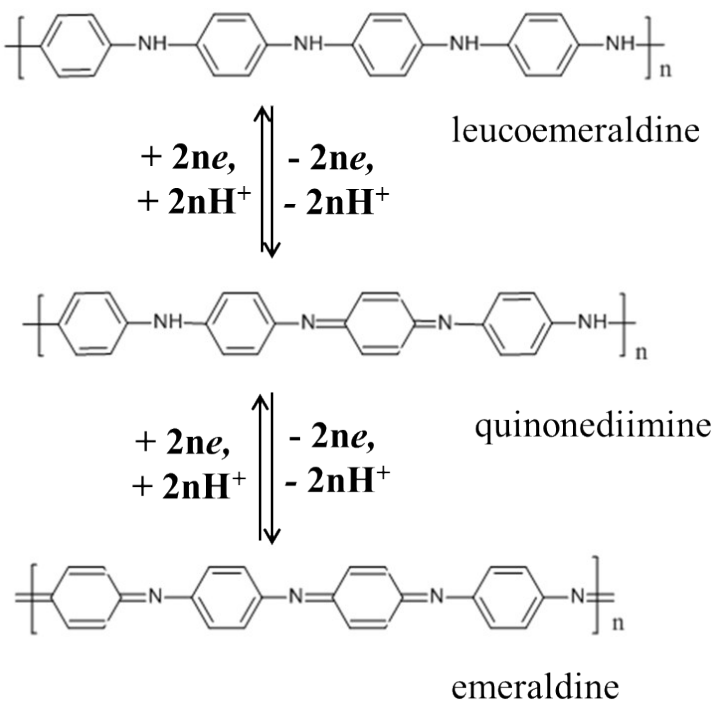

Figure S10. Equation of the redox reactions for PANI.

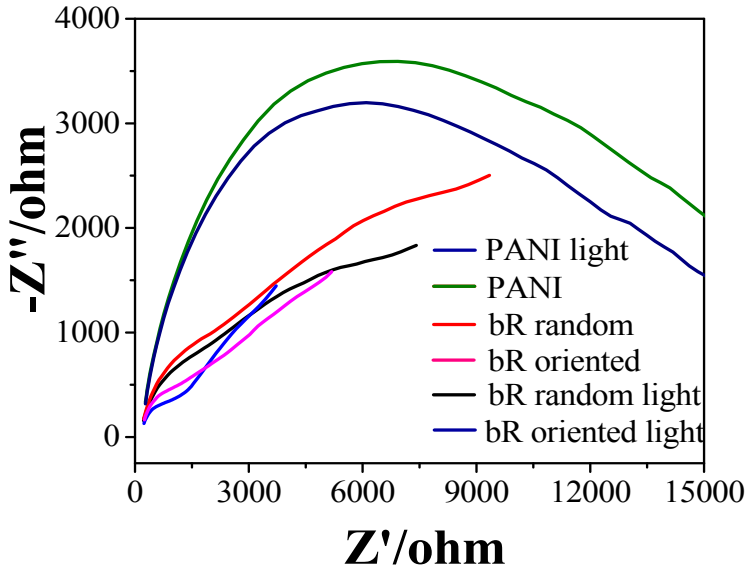

Figure S11. Nyquist plots of the bR/PANI and PANI electrodes in 0.1 M Na_2SO_4/H_2SO_4 solution (pH~ 5.0).

Table S1. Comparison of the capacitances of various supercapacitors fabricated based on polyaniline electroactive materials.

Material	Discharge Rate	Potential Range/V	Electrolyte	Specific Capacitance/F g^{-1}	Ref.
Polyaniline/Reduced Graphene Oxide Composite Electrode	53.33 A g^{-1}	0-0.8 V	1M H_2SO_4	808	3
PANI nanorod arrays / Expanded graphite nanosheets	8 A g^{-1}	0-0.8 V	1M H_2SO_4	836	4
Polyaniline–polyvinyl alcohol hydrogel	10 A g^{-1}	0-0.8 V	1M H_2SO_4	678	5
Compact Graphene–Polyaniline Hydrogel	50 A g^{-1}	0-0.9 V	1M H_2SO_4	About 480	6
PANI–CNT nanocomposites	5 A g^{-1}	0-0.8 V	1M H_2SO_4	430	7
bR / PANI	60 A g^{-1}	-0.2-0.8V	1 M H_2SO_4	1146	This work

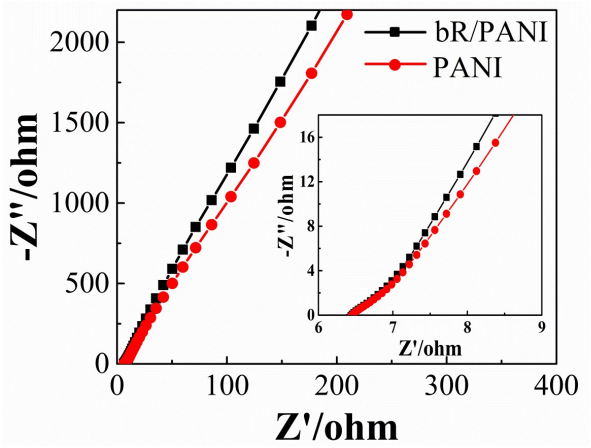

Figure S12. Nyquist plots of the bR/PANI and PANI electrodes.

References:

(1) Racker, E. Biochem. A new procedure for the reconstitution of biologically active phospholipid vesicles. *Biophys. Res. Commun.* **1973**, *55*, 224-230.

(2) Ayad, M. M., Salahuddin, N., Shenashin, M. A. Optimum reaction conditions for in situ polyaniline films. *Synth. Met.* **2003**, *132*, 185-190.

(3) Wu, J. F., Zhang, Q., Wang, J. J., Huang, X. P., Bai, H., A self-assembly route to porous polyaniline/reduced graphene oxide composite materials with molecular-level uniformity for high-performance supercapacitors. *Energy Environ. Sci.*, **2018**, *11*, 1280-1286.

(4) Li, Y. Z., Zhao, X., Yu, P. P., Zhang, Q. H., Oriented arrays of polyaniline nanorods grown on graphite nanosheets for an electrochemical supercapacitor. *Langmuir* **2013**, *29*, 493-500.

(5) Li, W. W., Gao, F. X., Wang, X. Q., Zhang, N., Ma, M. M. Strong and robust polyaniline-based supramolecular hydrogels for flexible supercapacitors. *Angew. Chem. Int. Ed.* **2016**, *55*, 9196-9201.

(6) Wang, Y. F., Yang, X. W., Pandolfo, A. G., Ding, J., Li, D. High-rate and high-volumetric capacitance of compact grapheme-polyaniline hydrogel electrodes. *Adv. Energy Mater.* **2016**, 1600185.

(7) Li, Y., Fang, Y. Z., Liu, H., Wu, X. M., Lu, Y., Free-standing 3D polyaniline–CNT/Ni-fiber hybrid electrodes for high-performance supercapacitors. *Nanoscale*, **2012**, *4*, 2867-2869.